DOI:10.3969/j.issn.1005-202X.2017.06.013

医学影像物理

$^{99m}TcO_4^-$显像与MRI和CT对比评价腮腺Warthin's瘤的诊断价值

张晓辉[1],彭祖光[1],李永明[1],曹贤东[2],刘永辉[3],唐颖豪[1],石有远[1],龙贵珍[1]
1.肇庆市第一人民医院核医学科,广东 肇庆 526021;2.肇庆市第一人民医院信息科,广东 肇庆 526021;3.肇庆市第一人民医院放射科,广东 肇庆 526021

【摘 要】**目的:**对比分析$^{99m}TcO_4^-$唾液腺显像与常规MRI和CT在评价腮腺Warthin's瘤中的准确性。**方法:**对78例临床疑诊腮腺Warthin's瘤的患者进行$^{99m}TcO_4^-$唾液腺显像,同时对其中61例患者进行腮腺CT或MRI检查(以下简称常规检查组),与病理结果进行对照,分别得出各自的诊断效能。采用受试者工作特征曲线对比分析$^{99m}TcO_4^-$唾液腺显像组与常规检查组诊断的准确性,并用χ^2检验对比两组的诊断效能。**结果:**$^{99m}TcO_4^-$唾液腺显像的灵敏度、特异性、阳性预测值、阴性预测值分别为94.12%、85.19%、92.31%、88.46%,常规检查组的灵敏度、特异性、阳性预测值、阴性预测值分别为28.26%、53.33%、65.00%、19.51%,两者差异有统计学意义(P<0.05)。受试者工作特征曲线中$^{99m}TcO_4^-$唾液腺显像组的曲线下面积为0.929,常规检查组的曲线下面积为0.496。**结论:**$^{99m}TcO_4^-$唾液腺显像诊断腮腺Warthin's瘤准确性高,有重要的临床应用价值。

【关键词】$^{99m}TcO4^-$;唾液腺显像;腮腺;Warthin's瘤;SPECT
【中图分类号】R445.5;R739.87 【文献标志码】A 【文章编号】1005-202X(2017)06-0603-04

Comparison of $^{99m}TcO_4^-$ imaging and MRI or CT examination in the diagnosis of parotid Warthin's tumor

ZHANG Xiaohui[1], PENG Zuguang[1], LI Yongming[1], CAO Xiandong[2], LIU Yonghui[3], TANG Yinghao[1], SHI Youyuan[1], LONG Guizhen[1]
1. Department of Nuclear Medicine, Zhaoqing First People's Hospital, Zhaoqing 526021, China; 2. Department of Information, Zhaoqing First People's Hospital, Zhaoqing 526021, China; 3. Department of Radiology, Zhaoqing First People's Hospital, Zhaoqing 526021, China

Abstract: Objective To compare and analyze the accuracy of $^{99m}TcO_4^-$ salivary gland imaging and conventional examinations (MRI and CT) in the diagnosis of parotid Warthin's tumor. **Methods** Among the 78 patients with suspected Warthin's tumor in the parotid gland who were treated with $^{99m}TcO_4^-$ salivary gland imaging, 61 patients underwent parotid gland CT or MRI examinations (conventional examination group). The results of $^{99m}TcO_4^-$ salivary gland imaging and conventional examination were compared with pathological results to obtain the diagnostic efficiency. The diagnosis accuracy of $^{999m}TcO_4^-$ salivary gland imaging group and conventional examination group were analyzed with receiver operating characteristic (ROC) curve, and the diagnostic efficiency of the two groups was compared with χ^2 test. **Results** The sensitivity, specificity, positive predictive value and negative predictive value of $^{99m}TcO_4^-$ salivary gland imaging group were 94.12%, 85.19%, 92.31% and 88.46%, respectively, and those of conventional group were 28.26%, 53.33%, 65.00% and 19.51%, respectively, with statistical significance between the two groups (P<0.05). The area under the ROC curve in $^{99m}TcO_4^-$ salivary gland imaging group and conventional examination group was 0.929 and 0.496, respectively. **Conclusion** Compared with conventional examination, $^{99m}TcO_4^-$ salivary gland imaging achieves higher accuracy on the diagnosis of Warthin's tumor in the parotid gland.

Keywords: $^{99m}TcO_4^-$; salivary gland imaging; parotid gland; Warthin's tumor; SPECT

前 言

腮腺Warthin's瘤是来源于腺体内淋巴结或残存临近淋巴结内的异位涎腺组织,是仅次于多形性腺瘤而居第2位的腮腺良性肿瘤,发病率为5%~10%,最近有上升趋势[1]。该疾病与免疫功能减退、吸烟及EB病毒感染有关。常规影像学检查特异性差,常被误诊为腮腺多形性腺瘤。以手术治疗为首要手段,手术方式与多形性腺瘤及其他腮腺肿瘤不同,因腮腺Warthin's瘤多发生于腮腺后下极,与腮腺实质关

【收稿日期】2017-03-13
【基金项目】肇庆市科技局基金(2012E282)
【作者简介】张晓辉,硕士,副主任医师,研究方向:头颈部影像学诊断,E-mail: 48555775@qq.com

系较松散，且其包膜完整，不会恶变，可单纯采用肿瘤摘除术，而腮腺多形性腺瘤因发生在腮腺实质内，并与腮腺实质关系密切，且包膜常不完整，术后易复发，可发生恶变，常采用腮腺浅叶扩大切除术[2]。因此，术前诊断准确，对于术式的选择及预后至关重要，本文探讨$^{99m}TcO_4^-$显像与MRI和CT对比评价腮腺Warthin's瘤的诊断价值。

1 资料与方法

1.1 临床资料

选取肇庆市第一人民医院2009年8月至2016年5月间临床疑诊腮腺Warthin's瘤的患者95例，其中78例符合纳入标准。纳入标准[3]：临床无痛性颌下肿块，术前1周进行$^{99m}TcO_4^-$唾液腺显像，并有病理资料。11例单独进行$^{99m}TcO_4^-$唾液腺显像，16例同时进行CT及$^{99m}TcO_4^-$唾液腺显像检查，45例同时进行MRI及$^{99m}TcO_4^-$唾液腺显像检查，并按检查方式分为$^{99m}TcO_4^-$唾液腺显像组78例，常规检查组61例（CT及MRI）。男性69例，女性9例。年龄14~79岁，平均（53.59±12.44）岁。

1.2 仪器与方法

SIEMENS ECAM双探头SPECT，矩阵128×128，低能平行孔准直器，能峰140 keV。药物来自广东希埃医药有限公司，放化纯度>95%。患者取仰卧位，探头紧贴患者头颈部，静脉注射$^{99m}TcO_4^-$，5 mci，动态采集26 min，1 min/帧。在采集20 min时含服维生素C 500 mg。采集完毕后行前位、侧位静态采集，并行体表结节定位。

GE公司1.5 T超导MRI，型号Signa Hde，使用头颈线圈，矩阵256×256，层厚4~5 mm，层距1 mm。采用横断位、冠状位及矢状位T_1W1及T_2W2采集和压脂采集后行对比剂增强。增强对比剂扎喷替酸葡甲胺，经肘静脉高压注射器注射，0.1 mmol/kg，流速0.2 mL/s。

GE公司64层螺旋CT，型号Light Speed。患者仰卧位，扫描范围为蝶窦至下颌角，120 keV，300 Mas，层厚1 mm，间隔0.8 mm，矩阵512×512，准直器宽度0.625 mm，螺距因子0.703。对比剂为非离子型碘化醇，采用双筒高压注射器，以5 mL/s注射流率，经右肘静脉团注（370 mgI/mL）80~100 mL。

1.3 影像诊断标准

1.3.1 $^{99m}TcO4^-$显像结果判读 图像由两位有经验的核医学医生共同分析。腮腺结节处放射性分布高于周围腺体，为“热结节”，包括酸刺激前后均为“热结节”表现和酸刺激前“温结节”表现而酸刺激后“热结节”表现，视为阳性结果[4]。

1.3.2 MRI结果判读 图像由2位放射科医生共同分析。平扫T_2WI/TSE呈不均匀低、稍高混杂信号，T_1WI/SE为低或稍低混杂信号，增强后实性部分轻-中度强化[5]。

1.3.3 CT结果判读 图像由两位放射科医生共同分析。稍高密度软组织结节，可有囊性成分，增强扫描实性部分呈中度以上强化[6-7]。

1.4 统计学方法

采用SPSS 19.0软件对所有数据进行统计分析，$^{99m}TcO_4^-$显像及常规检查对Warthin's瘤的诊断效能比较采用χ^2检验，$P<0.05$有统计学意义。以病理诊断作为“金标准”，通过绘制ROC曲线评价$^{99m}TcO_4^-$唾液腺显像组及常规检查组对Warthin's瘤的诊断价值。

2 结 果

78例患者共检出52例Warthin's瘤，多形性腺瘤16例，淋巴结炎症反应性增生5例，鳃裂囊肿3例，腺泡癌1例，粘液囊肿伴炎症1例。52例Warthin's瘤中瘤体大小1.1 cm×1.1 cm到4.6 cm×2.4 cm，12例（23.1%）为多发病灶，其中1例腮腺、下颌区、胸锁乳头肌均有病灶。根据受试者工作特征曲线，$^{99m}TcO_4^-$唾液显像组的曲线下面积为0.929（0.898±0.050，95% CI：0.799~0.996），明显高于常规检查组的0.496（0.457±0.082，95% CI：0.295~0.618）。

$^{99m}TcO_4^-$显像Warthin's瘤假阳性3例，均出现在患侧腮腺示踪剂排泄不良而出现“热结节”，2例位于腮腺中部，1例位于腮腺下极。3例假阴性的病例均发生在患侧腮腺摄取示踪剂功能下降的患者。常规检查组25例病理为Warthin's瘤的结节被判定为阴性，而腮腺$^{99m}TcO_4$-显像则判定为阳性，见图1和图2；常规检查组将4例多形性腺瘤、1例淋巴肉芽肿及1例淋巴结炎判定为阳性，而腮腺$^{99m}TcO_4$-显像判定为阴性。$^{99m}TcO_4^-$唾液显像诊断腮腺Warthin's瘤的灵敏度、特异性、阳性预测值、阴性预测值分别为94.12%、85.19%、92.31%、88.46%，常规检查组的灵敏度、特异性、阳性预测值、阴性预测值分别为28.26%、53.33%、65.00%、19.51%，两者差异具有统计学意义（$P<0.05$）。

3 讨 论

腮腺Warthin's瘤是良性肿瘤，常见于中老年男性患者，其中60%~70%有吸烟史[8]。病灶多位于腮腺下极，可为单发病灶或多发病灶，肿瘤大小1~4 cm，双侧腮腺均可受累，甚至发生于颌下腺和颈部。本研究中1例在腮腺、下颌区及胸锁乳突肌均见受累。

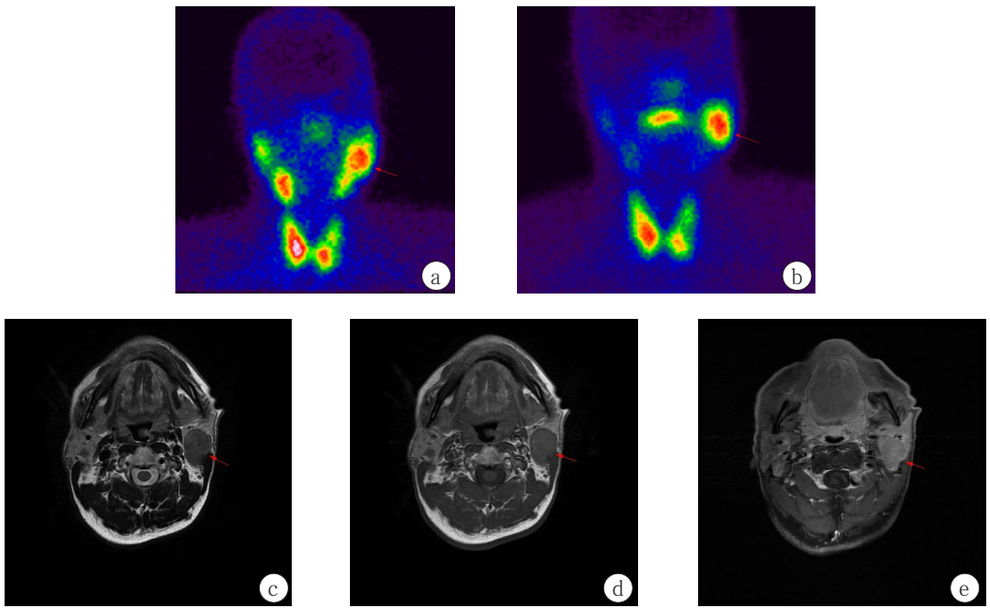

a: Early technetium-99m pertechnetate image showed increased uptake in the left parotid gland (hot nodules, red arrowhead); b: Late image with vitamin C stimulation also showed increased uptake in the same portion (hot nodules, red arrowhead) which was diagnosed of Warthin's tumor; c-e: The MRI image showed a soft tissue density shadow in the left parotid gland (red arrowheads); c: Lesion showed intermediate to low intensity on T_1-weighted image; d: Lesion shows intermediate intensity on T_2-weighted image; e: On the CE T_1-weighted image using the FS technique, lesion which showed an homogeneous enhancement was diagnosed of mixed tumor.

图1 $^{99m}TcO_4^-$显像诊断为Warthin′s瘤而MRI误诊为多形性腺瘤

Fig.1 Warthin′s tumor diagnosed with $^{99m}TcO_4^-$ imaging, and misdiagnosed of pleomorphic adenoma with magnetic resonance imaging

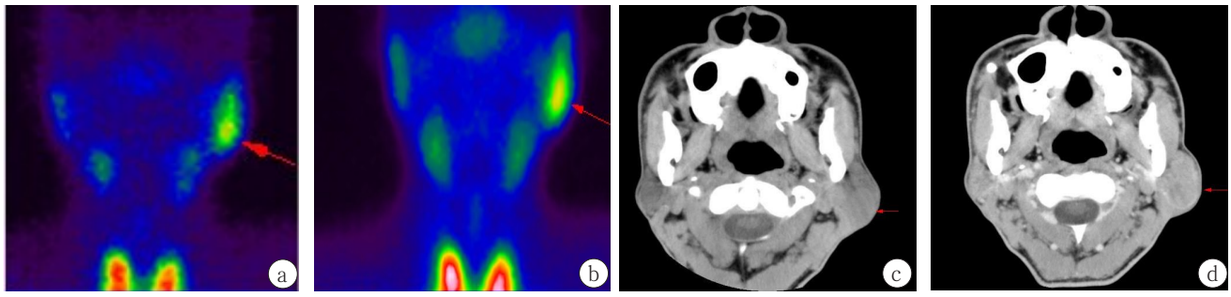

a: Early technetium-99m pertechnetate image showed increased uptake in the left parotid gland (hot nodules, red arrowhead); b: Late image with vitamin C stimulation also showed increased uptake in the same portion (hot nodules, red arrowhead) which was diagnosed of Warthin's tumor; c: The CT image showed a soft tissue density shadow in the left parotid gland with density uniform, clear boundary; d: After contrast medium administration, the tumor which showed an homogeneous enhancement on a CE CT image was diagnosed of mixed tumor.

图2 $^{99m}TcO_4^-$显像诊断为Warthin′s瘤而CT误诊为多形性腺瘤

Fig.2 Warthin′s tumor diagnosed with $^{99m}TcO_4^-$ imaging, and misdiagnosed of pleomorphic adenoma with CT

$^{99m}TcO_4^-$唾液腺显像可用于诊断腮腺Warthin's瘤[9-11],其摄取显像剂$^{99m}TcO_4^-$的机理是细胞膜内富含碘化钠同向转运体(NIS)[12]。NIS是一种质膜蛋白,普遍存在正常的甲状腺、哺乳期乳腺、胃和唾液腺组织,NIS可以促进组织摄取$^{99m}TcO_4^-$。Warthin's瘤和正常唾液腺组织都高摄取$^{99m}TcO_4^-$,但Warthin's瘤对$^{99m}TcO_4^-$的排泄不良而表现为“热结节”,多形性腺瘤等其他腮腺肿瘤不表达或较少表达NIS,所以图像表现为“温结节”或“冷、凉结节”。本研究中Warthin's瘤酸刺激前出现“热结节”32例,酸刺激后出现“热结节”18例,酸刺激后的18例中有16例表现为轻度摄取,而其中10例瘤体为1~2 cm。酸刺激前未出现“热结节”表现的原因可能为:(1)肿瘤体积较小,肿瘤体积与显像剂摄取程度呈正相关[13];(2)Warthin's瘤细

胞膜的NIS表达相对较少；(3)腮腺功能不良。以上原因可能导致酸刺激前Warthin's瘤摄取$^{99m}TcO_4^-$不高，而酸刺激后，正常腮腺组织将$^{99m}TcO_4^-$排泄，而Warthin's瘤不能排泄而表现为“热结节”。

本研究中$^{99m}TcO_4^-$显像Warthin's瘤假阳性3例，均出现在患侧腮腺示踪剂排泄不良而出现“热结节”，2例位于腮腺中部，1例位于腮腺下极，所以对图像中出现患侧腮腺示踪剂排泄不良应增加延迟显像，以提高诊断的准确性。3例假阴性的病例均发生在患侧腮腺摄取示踪剂功能下降的患者，可能原因为NIS表达不良，而导致$^{99m}TcO_4^-$摄取不良而漏诊；其余腮腺良性肿瘤本研究中均表现为“凉结节”。腮腺$^{99m}TcO_4^-$显像的灵敏度、特异性、阳性预测值和阴性预测值均明显高于常规的CT及MRI组，但$^{99m}TcO_4^-$显像对于腮腺Warthin's瘤的细节显示，如肿瘤的范围、位置及毗邻解剖等显示不良。

CT和MRI也常用于诊断腮腺肿瘤，二者均为解剖影像，可提供较好的解剖细节。随着MRI技术的飞速发展，MRI在鉴别肿瘤的良恶性中有较好的应用。Motoori等[14]报道MRI与$^{99m}TcO_4^-$显像相比在诊断腮腺肿瘤良恶性更有优势。CT及MRI诊断Warthin's瘤的主要依据为病灶发生位置、病灶数目、边缘情况，CT的密度可以均匀也可以不均匀，增强的强化程度不一，MRI T_1WI为低信号，T_2WI可以表现为低信号、中等信号甚至高信号，并因瘤体内成分不同而动态增强的类型也不尽相同[15-17]，导致图像无特异性，而出现该病诊断的灵敏性、特异性等不高，但CT及MRI能较好评估唾腺肿瘤的形态、大小和邻近结构的关系，也能在肿瘤良恶性鉴别中提供较好的诊断依据[18]。CT及MRI对腮腺内鳃裂囊肿的检出率较高，本研究中3例均检出。

总之，$^{99m}TcO_4^-$显像作为功能显像，在评价腮腺Warthin's瘤中仍有较好的诊断价值，可为临床医生进行术前定性诊断，如再结合CT或MRI的解剖结构及位置形态，可减少手术切除范围、降低手术并发症及保留腮腺大部分功能。

【参考文献】

[1] YU G, ZHOU Z, MA D, et al. Comprehensive study on the parotid Warthin tumor[J]. Chin J Stomatol, 1999, 34(3): 187-189.

[2] 杨安奎, 陈福进, 曾宗渊, 等. 腮腺沃辛瘤手术方式探讨[J]. 中国肿瘤, 2000, 9(11): 528-529.
YANG A K, CHEN F J, ZENG Z Y, et al. Clinical analysis of surgical treatment for parotid Warthin tumor[J]. China Cancer, 2000, 9(11): 528-529.

[3] OZAWA N, OKAMURA T, KOYAMA K, et al. Retrospective review: usefulness of a number of imaging modalities including CT, MRI, technetium-99m pertechnetate scintigraphy, Gallium-67 scintigraphy and F-18-FDG PET in the differentiation of benign from malignant parotid masses[J]. Radiat Med, 2006, 21(1): 41-49.

[4] 张晓辉, 彭祖光, 李永明, 等. $^{99m}TcO_4^-$唾液腺显像诊断腮腺腺淋巴瘤的应用价值[J]. 国际医药卫生导报, 2012, 18(9): 1232-1235.
ZHANG X H, PENG Z G, LI Y M, et al. Application value of $^{99m}TcO_4^-$ salivary gland scintigraphy on the diagnosis of papillary cystadenoma lymphomatosum[J]. International Medicine and Health Guidance News, 2012, 18(9): 1232-1235.

[5] 夏建东, 江新青, 彭国辉, 等. CT及MRI对腮腺腺淋巴瘤的诊断价值[J]. 实用放射学杂志, 2009, 5(9): 637-645.
XIA J D, JIANG X Q, PENG G H, et al. CT and MRI diagnosis of adenolymphoma of parotid gland[J]. Journal of Practical Radiology, 2009, 5(9): 637-645.

[6] 邱晓明, 王珍, 饶德利, 等. 腮腺腺淋巴瘤的CT诊断[J]. 医学影像学杂志, 2012, 22(1): 13-16.
QIU X M, WANG Z, RAO D L, et al. The CT diagnosis of parotid adenolymphomas[J]. Journal of Medical Imaging, 2012, 22(1): 13-16.

[7] 崔二峰, 张劲松, 唐永强. 腮腺Warthin瘤的CT诊断及鉴别诊断[J]. 中国临床医学影像杂志, 2017, 28(3): 169-172.
CUI E F, ZHANG J S, TANG Y Q. CT diagnosis and differential diagnosis of parotid Warthin tumor[J]. Journal of China Clinic Medical Imaging, 2017, 28(3): 169-172.

[8] PATEL D K, MORTON R P. Demographics of benign parotid tumors: Warthin's tumor versus other benign salivary tumors[J]. Acta Otolaryngol, 2016, 136(1): 83-86.

[9] MURATA Y, YAMADA I, UMEHARA I, et al. Diagnostic accuracy of technetium- 99m pertechnetate scintigraphy with lemon juice stimulation to evaluate Warthin's tumor[J]. J Nucl Med, 1998, 39: 43-46.

[10] WEINSTEIN G S, HARVEY R T, ZIMMER W, et al. Technetium-99m pertechnetate salivary gland imaging: its role in the diagnosis of Warthin's tumor[J]. J Nucl Med, 1994, 35: 179-183.

[11] 白槐延, 侯靖元, 解艳华, 等. 腮腺沃辛瘤切除术式的临床研究[J]. 广东牙病防治, 2009, 17(3): 133-134.
BAI H Y, HOU J Y, XIE Y H, et al. Clinical research of resection for parotid Warthin tumor[J]. Journal of Dental Prevention and Treatment, 2009, 17(3): 133-134.

[12] AKAI A, YAMAMURA Y K, NONAKA M, et al. $^{99m}TcO_4^-$ accumulation in scintigraphy and expression of Na^+/I symporter in salivary gland tumors[J]. Auris Nasus Larynx, 2014, 41(9): 532-538.

[13] MIYAKE H, MATSUMOTO A, HOFI Y E, et al. Warthin's tumor of parotid gland on Tc-99m perteehnetate scintigraphy with lemon juice stimulation: Tc-99m perteehnetate uptake, size, and pathologic correlation[J]. Eur Radiol, 2001, 11(12): 2472-2478.

[14] MOTOORI K, UEDA T, UCHIDA Y, et al. Identification of Warthin tumor magnetic resonance imaging *versus* salivary scintigraphy with Technetium-99m pertechnetate[J]. Comput Assist Tomogr, 2005, 29 (4): 506-512.

[15] YAO H Q, LIN H P, ZHANG P, et al. CT and MRI findings of parotid Warthin's tumors[J]. Chin-Germ J Clin Oncol, 2011, 10(10): 596-601.

[16] IKEDA M, MOTOORI K, HANAZAWA T, et al. Warthin tumor of the parotid gland: diagnostic value of MRI imaging with histopathologic correlation[J]. AJNR Am J Neuroradiol, 2004, 25(8): 1256-1262.

[17] LEE Y P, WONG K T, KING A D, et al. Imaging of salivary gland tumours[J]. Eur J Radiol, 2008, 11(6): 419-436.

[18] LIANG C H, DI W Y, REN J P, et al. Imaging, clinical and pathological features of salivary gland adenolymphoma[J]. Eur Rev Med Pharmacol Sci, 2014, 18: 3638-3644.

（编辑：黄开颜）